Resonant Raman scattering by acoustical phonons in Ge/Si self-assembled quantum dots: Interferences and ordering effects

M. Cazayous,* J. R. Huntzinger, J. Groenen, and A. Mlayah
Laboratoire de Physique des Solides, UMR 5477, Université P. Sabatier, 118 route de Narbonne, 31062 Toulouse Cedex 4, France

S. Christiansen and H. P. Strunk
Universität Erlangen-Nürnberg, Institut für Werkstoffwissenschaften-Mikrocharakterisierung, Cauerstraße 6, D-91058 Erlangen, Germany

O. G. Schmidt and K. Eberl
Max-Planck-Institut für Festkörperforschung, Heisenbergstraße 1, 70569 Stuttgart, Germany
(Received 25 February 2000)

We report on resonant Raman scattering by acoustical phonons in self-assembled Ge/Si quantum dot (QD) structures. Continuous emission is observed in the low frequency range for a single QD layer. This scattering is attributed to the breakdown of the wave vector conservation law due to the loss of translational invariance. In samples containing a stack of two Ge QD layers separated by a Si space layer, we observed a strong low frequency oscillating signal. We investigated the dependence of this signal on the spacing between the QD layers. Raman spectra were calculated, considering the deformation potential interaction between acoustical phonons and electronic states confined within the QD. These calculations account well for the experimental data and demonstrate that the oscillations are related to interferences between the QD layers. The effects of ordering and QD position correlation between layers on the interference contrast are discussed. It is shown that the experiments presented here provide an interesting means of probing electronic confinement and organization effects in QD structures.

I. INTRODUCTION

Three dimensional confinement of electrons and phonons in semiconductor quantum dots (QD's) has been extensively studied using such optical spectroscopy techniques as absorption, photoluminescence, and Raman scattering.[1] In most of the published work the experimental data are analyzed using a single QD picture. Many QD effects are usually ignored because in the case of diluted systems electron or phonon tunneling is negligible. Therefore, it is widely considered that a large ensemble of QD's behaves as an average QD and that fluctuations in QD size, shape, and position result only in inhomogeneous broadening of confined optical transitions as observed in light absorption and emission spectra. This assumption becomes questionable when electron–acoustic-phonon interaction is considered. Indeed, except for isolated particles where both electrons and phonons are confined within the QD, acoustic phonons can extend over many QD's providing the QD and barriers have similar mechanical properties. In other words, the coherence length of acoustic phonons can be comparable to the average distance between QD's if scattering of sound waves, due to fluctuations of the acoustic impedance at the QD/matrix interface, is weak. In that case, the emission or absorption of a given acoustic mode via electron-phonon interaction implies many QD's. As a result, correlations in QD positions should be manifest in low frequency Raman spectra as intensity maxima and minima, due to interferences between the scattering amplitudes associated with each QD. This is well known for semiconductor superlattices (SL's) and multiple quantum well (MQW) structures where the superperiodicity leads to constructive interference only for acoustic phonons with Bragg wave vectors (diffraction).[2,3]

In this paper, we report on resonant Raman scattering by acoustical phonons in self-assembled QD structures. Most of the published Raman studies on self-assembled QD's were limited to the optical phonon frequency range.[4–8] It was demonstrated that valuable information about residual strain and chemical composition in the QD can be derived from the optical phonon Raman spectra.[4,6,7] Raman scattering by acoustic phonons in self-assembled QD's was reported very recently.[9–11] References 9 and 10 deal with structures containing many QD layers, and the corresponding low frequency Raman spectra display features similar to the ones observed in SL's. In Ref. 11 we reported acoustic phonon Raman scattering in structures containing a single layer of InAs/InP QD's. Periodic oscillations were observed and attributed to the interaction between confined electronic states and standing acoustic waves due to the reflection at the sample surface. The oscillation period was shown to depend greatly on the distance between the sample surface and the QD layer. The structures investigated here contain either one or two QD layers only. For the double QD layers we observe strong oscillations of the low frequency scattering, which we interpret as interferences between the Raman scattering amplitudes of each QD layer. Calculations based on the interaction of acoustic phonons with electronic states confined in the QD are compared to the experimental data. At first sight, the low frequency oscillations we observe can be understood in terms of short or finite size superlattice effects, similar to those reported by Dharma-wardana *et al.*[12] However, a detailed analysis of the Raman scattering process shows that the strain-induced vertical correlation of QD positions[13–15] is

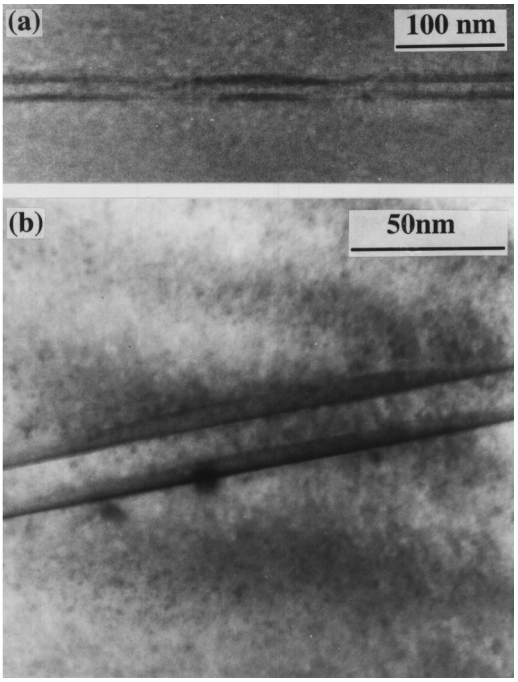

FIG. 1. Cross-sectional TEM images of sample *B* showing (a) two Ge QD layers and (b) a QD column along the growth direction. The images clearly demonstrate the vertical correlation between QD's.

a key feature for understanding our experimental findings.

The paper is organized as follows. After a brief description of the growth and experimental procedures, we present our low frequency Raman scattering data. Calculations are reported and compared to the experimental data. We finally discuss these results, with a special emphasis on QD ordering.

II. EXPERIMENTS

Ge QD layers embedded in Si(001) were grown by solid source molecular beam epitaxy at 700 °C. Details of growth have been reported in Ref. 16. Sample *A* contains a single QD layer obtained by a 5 monolayer (0.7 nm) Ge deposition on a 400 nm Si buffer layer and capped by a 160 nm Si layer. Samples *B*, *C*, and *D* contain two QD layers (each corresponding to the same deposition as sample *A*) separated by a Si interlayer. The interlayer thickness is 15, 30, and 60 nm for *B*, *C*, and *D*, respectively.

The structural characterization was performed by means of transmission electron microscopy (TEM) (conventional and high resolution). Figure 1 clearly demonstrates the self-alignment of the QD's. This vertical correlation was shown to originate in the strain field induced by the subjacent island in the Si layer and to depend on the interlayer thickness.[13–15] According to TEM, the actual interlayer thicknesses in samples *B*, *C*, and *D* differ slightly from the nominally intended ones. Indeed, TEM yields the following values for the spacing *d* (*d* includes the Si interlayer thickness and the 0.7 nm nominal Ge deposit): 16.8, 32.8, and 62 nm (with an accuracy of ± 1 nm) for samples *B*, *C*, and *D*, respectively. As shown in Fig. 1(b), the dots have the shape of flat, plano-convex lenses with a mean width *w* of about 170 nm. The dot height typically ranges from 7 to 8 nm.

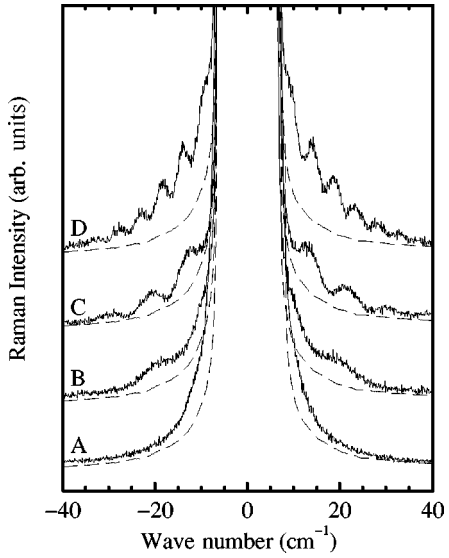

FIG. 2. Low frequency Raman spectra of samples *A*, *B*, *C*, and *D* (recorded with the 476 nm laser line at room temperature). The dashed lines are Si reference spectra.

Raman spectra were recorded in both optical and acoustical phonon frequency ranges at room temperature using several Ar^+ laser lines. The latter allow one to achieve excitation in resonance with the E_1 transition of the QD's. The scattered light was dispersed by a T800 Coderg triple spectrometer and detected with a photomultiplier. The incident angle of the laser beam was set close to the Brewster angle. Inside the samples the scattering configuration is close to the backscattering geometry due to the Si refractive index. Samples were kept in vacuum in order to avoid air related Raman peaks in the low frequency range. Reference spectra were systematically recorded on a bulk Si(001) sample. In this paper, we shall focus on Raman scattering by acoustical phonons. Let us briefly mention, however, the main result derived from the optical phonon spectra. These unambiguously indicate that Si has diffused into the Ge dots. Similar behavior has already been reported for high growth temperatures.[17,18] Following the procedure described in Ref. 4, we find a 70% Ge content in the dots.

Figure 2 shows low frequency Raman spectra recorded on samples *A*, *B*,*C*, and *D* with the 476 nm laser line. Si reference spectra are reported for comparison. The spectrum of sample *A* exhibits continuous emission centered on the Rayleigh scattering. In contrast with the monotonic variation observed for sample *A*, the spectra of samples *B*, *C*, and *D* display periodic oscillations in both Stokes and anti-Stokes regions. The oscillation period decreases when the spacing increases; the period for *B*, *C*, and *D* is 14.7, 8.4, and 4.7 cm^{-1}, respectively.

Figure 3 presents low frequency Raman spectra recorded on sample *C* with laser lines between 2.4 and 2.7 eV. Thanks to the small acoustic phonon energies, double resonance conditions are nearly fulfilled. This provides us with a strong low frequency signal as intense as the signal in the optical phonon frequency range (not shown here). The Raman intensity increases with the excitation energy. The available laser lines do not allow us to surround the resonance totally. Nevertheless, the E_1 transition is expected around 2.7 eV for

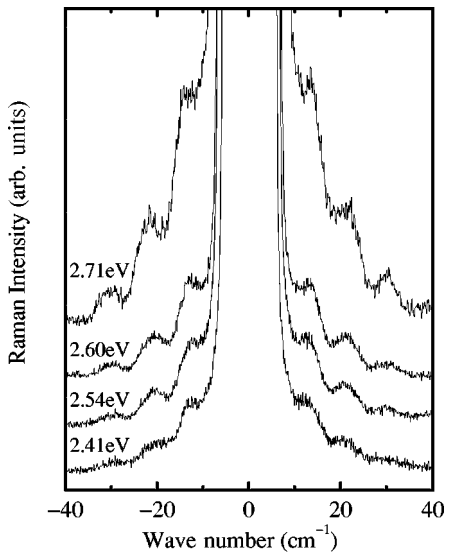

FIG. 3. Raman spectra of sample *C* recorded with excitation energies 2.41, 2.54, 2.60, and 2.71 eV around resonance with the E_1 transition.

70% Ge content.[19] Moreover, the oscillation period and spectral shape do not depend on the excitation energy in the range investigated. In fact, because the electrons and holes have large effective masses around the L point, the E_1 confinement-induced energy shifts are negligible.[19] Therefore, selective excitation of a particular E_1 sublevel is impossible at room temperature.

III. CALCULATIONS

In order to account for the low frequency continuous scattering and periodic oscillations, we use calculations based on the interaction between bulklike acoustic phonon modes and confined electronic states.

It has already been shown that localization of the electronic states involved at resonance induces breakdown of the wave vector conservation law in the Raman scattering process. As a result, scattering by phonon modes with wave vectors belonging to the whole Brillouin zone becomes allowed. In the acoustic phononfrequency range, this is manifest in the Raman spectra as a continuous scattering centered around the excitation line. Its spectral shape strongly depends on the electron (and hole) wave function as already shown for single and multiple two-dimensional quantum wells.[20–22]

In QD's one has in principle to consider both the confinement along the growth axis and the lateral confinement. However, due to the particular shape and size of the QD's investigated here (the dot diameter is about one order of magnitude larger than the dot height), we disregard the lateral confinement, and thus solely consider the nonconservation of the wave vector q_z along the growth axis. We shall reconsider this approximation and the effects related to the nonconservation of the in-plane component $q_\parallel$ below.

According to the experimental scattering geometry, the phonons involved in the scattering are longitudinal acoustic (LA) modes polarized along the growth axis.[22] We approximate the displacement field of LA phonons propagating along the growth direction by simple plane waves. Indeed, owing to the small acoustic impedance mismatch between Si and Ge and the small number (one or two) of QD layers, acoustic wave reflections at the Si/Ge interfaces can be disregarded here.[23] The amplitudes of propagating waves have been obtained by considering continuity conditions for the displacement field at the QD/Si interfaces. At a given frequency, the wave vector in each material (QD or Si) depends on the appropriate sound velocity. We consider a linear dispersion for the acoustical phonon frequencies. The QD (70% Ge) longitudinal sound velocity is interpolated from the longitudinal sound velocities in Si and Ge. According to Refs. 25 and 26, $v_{\mathrm{Si}}=9000\ \mathrm{m\,s^{-1}}$ and $v_{\mathrm{Ge}}=5000\ \mathrm{m\,s^{-1}}$.

We consider deformation potential electron-phonon interaction and calculate the coherent superposition of the scattering contributions from the two QD layers. We consider two QD's, each belonging to a different layer and located one above the other (this is equivalent to a double QW configuration, as lateral confinement is disregarded). Assuming that double resonance conditions are fulfilled, the Raman scattering intensity for acoustic phonon emission is proportional to[27,28]

$$\left| \sum_{l=1}^{2} \vec{q}\,\vec{u}_q \sqrt{n_q+1}\,\delta(\Delta\vec{k}_\parallel - \vec{q}_\parallel) \int e^{i(\Delta k_z - q_z)z} |\varphi_l(z)|^2 dz \right|^2, \tag{1}$$

where l is the QD layer index, $\vec{q}$ and $\vec{u}_q$ are the three-dimensional wave vector and amplitude of the propagating LA wave, n_q is the Bose-Einstein population factor and Δk_z ($\Delta\vec{k}_\parallel$) is the difference between the incident and scattered photon wave vectors along (perpendicular to) the growth axis. Considering solely $l=1$ or 2 allows one to calculate the single QD layer spectrum. Because we assume perfect two-dimensional QW's, the wave vector conservation law is fulfilled in the QW plane [$\delta(\Delta\vec{k}_\parallel - \vec{q}_\parallel)$ in Eq. (1)], whereas confinement along the growth direction results in nonconservation of q_z as denoted by the integral term in which $\varphi_l(z)$ is the confined electronic wave function. The latter is assumed to be totally confined within the QD (infinite barrier height) and described by a cosine function (first confined state).

IV. RESULTS AND DISCUSSION

Figure 4 shows the experimental spectra of the QD samples (the same as in Fig. 2) subtracted from the Si reference spectrum. Notice that, despite this subtraction, a significant Rayleigh signal remains. The Raman spectra calculated according to Eq. (1) are also shown. Calculations were performed with the same QD height $h=8$ nm for all samples. The values of the spacing d between the QD's (from center to center) used in the calculations (16.8, 31, and 60 nm for samples *B*, *C*, and *D*, respectively) are in good agreement with the ones determined by high resolution TEM. The calculated spectra were convoluted with the spectral response of our experimental setup (2 $\mathrm{cm^{-1}}$ resolution). Except for simple scaling factors, no other adjustable parameters were used.

Let us first discuss sample *A*. For the single QD layer, one obtains a continuous emission band. Its shape is mainly determined by the Fourier transform of the probability density $|\varphi(z)|^2$ [Eq. (1)]. Therefore, the spectral shape of the con-

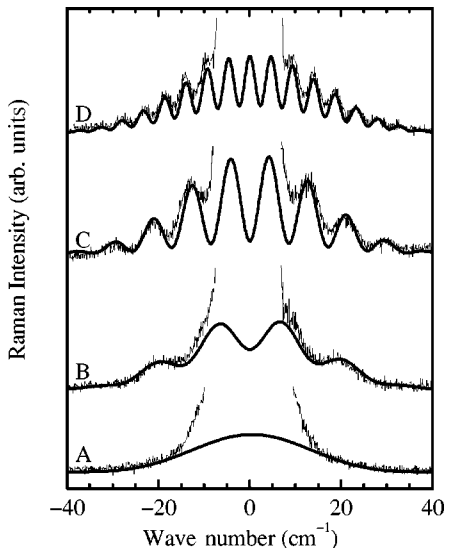

FIG. 4. Experimental and calculated low frequency Raman spectra of samples *A*, *B*, *C*, and *D*. A Si reference spectrum was subtracted from the experimental ones.

tinuous emission depends greatly on the electron confinement in the QD, i.e., the QD height. These results are similar to the ones reported for single QW's.[20–22] Unfortunately, the remaining Rayleigh signal hinders comparison with the experimental spectrum.

For structures containing two QD layers (samples *B*, *C*, and *D*), strong periodic oscillations are obtained. They originate from the coherent superposition of the scattering amplitudes associated with each QD layer. The maxima and minima correspond to constructive and destructive interferences, respectively. The oscillation period is determined by the spacing d and the sound velocities in the QD and Si barriers. The model accounts quantitatively for the oscillation dependence on spacing. As expected, the oscillation period decreases with increasing d. The spectral envelope of the oscillating signal (samples *B*, *C*, and *D*) is the continuous emission spectrum calculated for the single QD layer (sample *A*). The good agreement with experiment confirms that the parameters we used ($h=8$ nm and a 70% Ge content) are appropriate. Notice that we considered the contribution of the first confined state only. In principle, excited states should be taken into account. As pointed out above, we cannot selectively excite particular confined states (in contrast with resonant excitation measurements performed[20,22] on MQW's). However, we found that the spectral shape of the low frequency scattering obtained by summing the contributions of many confined levels is very similar to the one presented here. This sum is equivalent to considering a uniform electronic distribution density within the QD. The Fourier transform of this uniform distribution is similar to that of the first confined state.

At this stage one may wonder whether standing acoustic wave effects, like those reported in Ref. 11, are important here. Indeed, standing waves, extending into all the layers, may result from the superposition of two counterpropagating waves ($q_z<0$ and $q_z>0$) due to the total reflection (100%) at the sample surface. According to the Si cap layer thickness (160 nm), interaction between the confined electronic states and standing acoustic waves (instead of plane waves) would result in an additional small oscillation period of ≈ 0.8 cm^{-1}. The spectral envelopes of this rapidly oscillating signal are the calculated spectra in Fig. 4. However, these additional oscillations (if present) cannot be resolved with our experimental setup despite its high resolution: one would observe only their envelope (i.e., our calculations).[29] From an experimental point of view, we are thus not able to address here whether or not the QD layers experience standing acoustic waves. We did not include them in the calculations therefore.

Moreover, acoustic wave reflections at the Ge/Si interfaces were disregarded. If included, however, they would not change significantly the spectra presented in Fig. 4 because of the very small reflection coefficient ($\approx 1\%$) and the few interfaces in our structures. For structures with many interfaces one has to take these reflections into account. As a matter of fact, it is well known that periodic doublet peaks are observed in the low frequency Raman spectra of superlattices and multiple quantum wells. Their period depends on the sound velocities and the thicknesses of the layers, whereas the doublet splitting arises from interferences between partially reflected and transmitted waves at the many interfaces.

Let us now discuss the interference contrast. The model accounts well for that observed for sample *B*. However, for samples *C* and *D*, it predicts more pronounced oscillations than those obtained experimentally. As a matter of fact, the double QW configuration considered in the calculations (two QD's one above the other, no lateral confinement) gives the maximum contrast. Notice, however, that the calculated spectra display nonzero minima. This is caused by three effects that were taken into account in the calculations: (i) the finite spectral resolution; (ii) light absorption in the QD and Si interlayer; (iii) the frequency shift between the contributions of the acoustic waves propagating toward the substrate ($q_z<0$) and toward the surface ($q_z>0$). These contributions are considered independently: $I(\omega=v|q_z|)=I(-q_z)+I(q_z)$ (no interferences). Their shift depends on $\Delta k_z d$ (modulo π). (i) and (ii) only slightly reduce the oscillation contrast, whereas (iii) leads to a rather low calculated contrast for sample *B* (Fig. 4).

At this stage, to discuss further contrast, we should reconsider the lateral electronic confinement in the QD's. As already mentioned above, it induces nonconservation of the in-plane crystal momentum component $q_\parallel$ in the scattering. The continuous emission spectrum thus depends also on the QD width. In our case, as the width is much larger than the height, the spectral shape of the continuous emission spectrum is not modified much, except close to $\omega=0$. Indeed, as the envelope depends on the activated phonon density of states, for small wave numbers the continuous intensity should increase linearly with ω for a three-dimensional dispersion [calculations based on a one-dimensional dispersion $\omega=vq_z$ give a flat scattering intensity at $\omega_{q_z}=0$ (Fig. 4)].[22] Notice, however, that because of the Rayleigh scattering we cannot address this experimentally.

Within a single QD layer, one has to consider the superposition of the scattering contributions originating from all the QD's. However, as the QD's are not ordered within the plane, no well defined phase relationship exists between the

QD's. Therefore, we do not expect interference effects to appear in the Raman spectra (spectrum *A* in Fig. 4).

The interference contrast in a double QD layer depends on the in-plane QD positions but also on the relative inter-plane QD positions. To point out these dependencies we shall adopt the following simplified model. We consider a double QD layer, the QD's being all identical (same size, same single electronic state). Their location is given by $\vec{r}_{j_l}$ where j and l are the QD and layer index, respectively. Assuming that acoustic phonons can be described by plane waves $e^{i\vec{q}\cdot\vec{r}}$ with isotropic dispersion, the Raman intensity is proportional to

$$[S_{11}(\vec{q}_\parallel)+S_{22}(\vec{q}_\parallel)]\left[1+\mathrm{Re}\left(e^{iq_z d}\frac{2S_{12}(\vec{q}_\parallel)}{S_{11}(\vec{q}_\parallel)+S_{22}(\vec{q}_\parallel)}\right)\right], \tag{2}$$

where

$$S_{ll'}(\vec{q}_\parallel)=\sum_{j_l,j'_{l'}} e^{i\vec{q}_\parallel\cdot(\vec{r}_{j_l}-\vec{r}_{j'_{l'}})}. \tag{3}$$

$S_{11}(\vec{q}_\parallel)$ and $S_{22}(\vec{q}_\parallel)$ are structure factors related to the spatial correlation of the QD positions within layers 1 and 2, respectively, while $S_{12}(\vec{q}_\parallel)$ is determined by the correlations in QD positions between layers 1 and 2. As can easily be identified in Eq. (2), the interference contrast is given by $2S_{12}/(S_{11}+S_{22})$. When the quantum dots have identical positions in both layers (perfect correlation) $S_{12}=S_{11}=S_{22}$ and the contrast is maximum.

For random (and different) distributions of the QD's in each layer $S_{11}=S_{22}=N$, where N is the number of QD's (per layer) under the laser spot. In that case S_{12} is vanishing except for $q_\parallel(r_{j_1}-r_{j'_2})\ll 1$. Assuming $q_\parallel\simeq\pi/w$, w being the average QD width, $q_\parallel(r_{j_1}-r_{j'_2})\ll 1$ means that the in-plane separation between QD's j_1 and j'_2 is much smaller than the average dot size. Then the two quantum dots can be considered as located one above the other (i.e., separated by d), which gives nonzero values for S_{12} and thus a nonvanishing contrast. So, for given QD distributions in each layer, one has to estimate how many QD's are vertically aligned. If the distributions are random one can show that this number is about $N(w/\bar{l})^2$, where $\bar{l}$ is the average distance between QD's. Then the contrast should be maximum for high QD densities $\bar{l}\simeq w$ and should vanish for diluted systems $\bar{l}\gg w$.

The average width w deduced from our TEM measurements is 170 nm. According to atomic force microscopy measurements,[16] the average distance $\bar{l}$ is about 300 nm. So, if we assume random distributions of the QD's in each layer, the contrast should be reduced by about 70% with respect to the double quantum well configuration (solid lines in Fig. 4). The comparison between calculated and measured Raman spectra presented in Fig. 4 clearly shows that the observed interference contrast is larger. As mentioned above, the double quantum well configuration assumed in the calculations gives the maximum contrast since the in-plane distribution of the electronic densities in both QW's is uniform and therefore perfectly correlated. The strong interference contrast we observe is thus inconsistent with uncorrelated random distributions of the QD's within each layer. In fact, TEM measurements demonstrate the vertical QD position self-alignment in our samples. Therefore the strong oscillation contrast of the low frequency Raman spectra obtained on our double QD layers is likely the signature of QD ordering along the growth axis. According to their spacing, samples *B*, *C*, and *D* have a high degree of position alignment (see Ref. 15). For larger spacings[15] ($d>100$ nm) we expect the contrast to decrease.

In our discussion, we assume two layers with identical QD's (size and composition). Size fluctuations should lower the interference contrast. In fact, recent photoluminescence data[16] show that the QD Ge content could be slightly different in the two layers. This difference would also reduce the interference contrast. As a matter of fact, however, according to the compositional and size dependencies of the E_1 gap, these effects should be weak. It is worth emphasizing that, despite all possible differences between QD's, we observe an interference contrast almost as strong as in the double-QW case (i.e., the correlated dot case).

V. CONCLUSION

Nonconservation of crystal momentum is a key feature for resonant Raman scattering in low dimensional structures, i.e., those involving localized electronic states. Indeed, due to the lack of translational invariance, acoustical phonons are Raman active.

We observed the corresponding continuous emission in resonant Raman spectra of a single QD layer structure. Its spectral shape was shown to depend on size and dimensionality, i.e., electronic confinement. We showed that interferences occur in the acoustical phonon frequency range for double QD layer structures. The interference oscillation period is determined by the spacing between the layers and the envelope corresponds to the continuous emission observed for a single QD layer.

These interferences are observed because our samples exhibit vertical QD position self-alignment. The interference contrast indeed depends on the QD position correlation between layers: it is maximum for perfect correlation. Resonant Raman scattering thus offers an interesting means of probing self-organization effects in QD layer structures. We predict significant changes in the low frequency Raman spectra to occur as a function of QD self-organization in plane and/or along the growth direction.

*Email address: cazayous@ramansco.ups-tlse.fr

[1] For a review, see U. Woggon, *Optical Properties of Semiconductor Quantum Dots*, Vol. 136 of *Springer Tracts in Modern Physics*, edited by G. Höhler (Springer-Verlag, Berlin, 1997).

[2] C. Colvard, R. Merlin, M.V. Klein, and A. Gossard, Phys. Rev. Lett. **45**, 298 (1980).

[3] B. Jusserand, F. Alexandre, J. Dubard, and D. Paquet, Phys. Rev. B **33**, 2897 (1986).

[4] J. Groenen, R. Carles, S. Christiansen, M. Albrecht, W. Dorsch, H.P. Strunk, H. Wawra, and G. Wagner, Appl. Phys. Lett. **71**,

3856 (1997).
[5] P.D. Persans, P.W. Deelman, K.L. Stokes, L. Schowalter, A. Byrne, and T. Thundat, Appl. Phys. Lett. **70**, 472 (1997).
[6] S.H. Kwok, P.Y. Yu, C.H. Tung, Y.H. Zhang, M.F. Li, C.S. Peng, and J.M. Zhou, Phys. Rev. B **59**, 4980 (1999).
[7] J. Groenen, C. Priester, and R. Carles, Phys. Rev. B **60**, 16 013 (1999).
[8] A.A. Sirenko, M.K. Zundel, T. Ruf, K. Eberl, and M. Cardona, Phys. Rev. B **59**, 4980 (1999).
[9] J.L. Liu, G. Jin, Y.S. Tang, Y.H. Luo, K.L. Wang, and D.P. Yu, Appl. Phys. Lett. **76**, 586 (1999).
[10] D.A. Tenne, V.A. Haisler, A.I. Toropov, A.K. Bakarov, A.K. Gutakovsky, D.T.A. Zahn, and A.P. Shebanin, Phys. Rev. B **61**, 13 785 (2000).
[11] J.R. Huntzinger, J. Groenen, M. Cazayous, A. Mlayah, N. Bertru, C. Paranthoen, O. Dehaese, H. Carrère, E. Bedel, and G. Armelles, Phys. Rev. B **61**, R10 547 (2000).
[12] M.W.C. Dharma-wardana, P.X. Zhang, and D.J. Lockwood, Phys. Rev. B **48**, 11 960 (1993).
[13] Q. Xie, A. Madhukar, P. Chen, and N.P. Kobayashi, Phys. Rev. Lett. **75**, 2542 (1995).
[14] J. Tersoff, C. Teichert, and M.G. Lagally, Phys. Rev. B **76**, 1675 (1996).
[15] O. Kienzle, F. Ernst, M. Rühle, O.G. Schmidt, and K. Eberl, Appl. Phys. Lett. **74**, 269 (1999).
[16] O.G. Schmidt and K. Eberl, Phys. Rev. B **61**, 13 721 (2000).
[17] T.I. Kamins, G. Medeiros-Ribeiro, D.A.A. Ohlberg, and R.S. Williams, J. Appl. Phys. **85**, 1159 (1999).
[18] J. Zhu, C. Miesner, K. Brunner, and G. Abstreiter, Appl. Phys. Lett. **75**, 2395 (1999).
[19] T.P. Pearsall, F.H. Pollak, J.C. Bean, and R. Hull, Phys. Rev. B **33**, 6821 (1986).
[20] V.F. Sapega, V.I Belitsky, A.J. Shields, T. Ruf, M. Cardona, and K. Ploog, Solid State Commun. **84**, 1039 (1992).
[21] A. Mlayah, A. Sayai, R. Grac, A. Zwick, R. Carles, M.A. Maaref, and R. Planel, Phys. Rev. B **56**, 1486 (1997).
[22] T. Ruf in *Phonon Raman Scattering in Semiconductors, Quantum Wells and Superlattices*, Vol. 142 of, *Springer Tracts in Modern Physics*, edited by G. Höhler (Springer-Verlag, Berlin, 1998).
[23] η is the acoustic impedance mismatch between Si and Ge i.e., $\eta=\rho_{\mathrm{Si}}v_{\mathrm{Si}}/\rho_{\mathrm{Ge}}v_{\mathrm{Ge}}$, where ρ_{Si} (ρ_{Ge}) and v_{Si} (v_{Ge}) are the crystal density (Ref. 24), and sound velocity (Refs. 25 and 26) in Si (Ge). We get $\eta=0.78$. The corresponding acoustical reflection coefficient is 0.014.
[24] L. Reggiani, *Hot Electron Transport in Semiconductors* (Springer-Verlag, Berlin, 1985).
[25] J. Kulda, D. Strauch, P. Pavone, and Y. Ishii, Phys. Rev. B **50**, 13 347 (1994).
[26] G. Nilsson, and G. Nelin, Phys. Rev. B **6**, 3777 (1972).
[27] V.I. Belitsky, T. Ruf, J. Spitzer, and M. Cardona, Phys. Rev. B **49**, 8263 (1994).
[28] T. Ruf, J. Spitzer, V.F. Sapega, V.I. Belitsky, M. Cardona, and K. Ploog, Phys. Rev. B **50**, 1792 (1994).
[29] In Ref. 11, the distance between the single layer of QD's and the sample surface ranged from 10 to 20 nm, providing a large, and thus observable, oscillation period ranging from 13 to 5 cm^{-1}. Owing to the thick Si cap layer (160 nm), these standing wave effects are not observed here (see, for instance, the spectrum of the single QD layer, Fig. 4).